

In-medium properties of a ΞN interaction derived from chiral effective field theory

J. Haidenbauer¹ and U.-G. Meißner^{2,1,3}

¹Institute for Advanced Simulation, Institut für Kernphysik (Theorie) and Jülich Center for Hadron Physics, Forschungszentrum Jülich, D-52425 Jülich, Germany

²Helmholtz Institut für Strahlen- und Kernphysik and Bethe Center for Theoretical Physics, Universität Bonn, D-53115 Bonn, Germany

³Tbilisi State University, 0186 Tbilisi, Georgia

Received: date / Revised version: date

Abstract. The in-medium properties of a baryon-baryon interaction for the strangeness $S = -2$ sector derived within chiral effective field theory up to next-to-leading order are investigated. The considered ΞN interaction is in line with available empirical constraints on the $\Lambda\Lambda$ S -wave scattering length and on ΞN elastic and inelastic cross sections. In particular, there are no near-threshold bound states in the ΞN system. A conventional G -matrix calculation for this interaction is performed and reveals that the single-particle potential of the Ξ -hyperon in nuclear matter is moderately attractive as suggested by recent experimental evidence for the existence of Ξ -hypernuclei.

PACS. 12.39.Fe Chiral Lagrangians – 13.75.Ev Hyperon-nucleon interactions – 21.30.Fe Forces in hadronic systems and effective interactions

1 Introduction

A few years ago a hyperon-nucleon (YN) interaction has been derived up to next-to-leading order (NLO) in chiral effective field theory (EFT) by the Jülich-Bonn-Munich group [1] and soon afterwards an extension to baryon-baryon (BB) systems with strangeness $S = -2$ ($\Lambda\Lambda$, $\Sigma\Sigma$, ΞN) [2] was presented. An excellent description of available ΛN and ΣN scattering data could be achieved at NLO [1]. With regard to the $S = -2$ sector, the situation was much less conclusive simply because of the scarcity of pertinent scattering data for the $\Lambda\Lambda$, $\Sigma\Sigma$ and ΞN systems. Indeed, there are just a few data points and upper bounds for the ΞN elastic and inelastic cross sections [3, 5, 4] that put constraints on the corresponding interactions. Those constraints were met by the interaction proposed in Ref. [2]. However, it was also admitted that a quantitative determination of the $S = -2$ BB interaction and, thus, of key quantities like scattering lengths was not possible due to the lack of more stringent experimental information.

In the present paper we revisit the ΞN interaction within chiral EFT. Though, unfortunately, there is no new information on the elementary ΞN observables, other developments over the last few years make this worthwhile. First, now there are stronger indications that bound Ξ -hypernuclei could indeed exist. Specifically, evidence for deeply bound states in systems like Ξ^- - ^{14}N [6] (Kiso event) or Ξ^- - ^{11}B [7, 8] have been reported. Second, there is still an ongoing discussion about the role that hyper-

ons play for the size and stability of neutron stars. This concerns first of all the Λ hyperon, but also the Ξ [9, 10, 11, 12, 13, 14]. Third, the possibility to extract information on the ΞN interaction from studying the pertinent correlations in heavy-ion collisions and/or high energetic pp collisions might become feasible soon [16, 15, 17]. Finally, results from lattice QCD simulations for the ΞN interaction have become available for masses very close to the physical point [18, 19, 20].

The results presented in Ref. [2] suggest that the ΞN interaction has to be relatively weak in order to be in accordance with the available empirical information. In particular, the published values and upper bounds for the Ξ^-p elastic and inelastic cross sections [5, 4] practically rule out a somewhat stronger attractive ΞN force and, specifically, disfavor any near-threshold deuteron-like bound states in that system that were predicted by various phenomenological potentials in the past [21, 22]. However, it remained open in how far such a very weakly attractive ΞN interaction like that in Ref. [2] is compatible with in-medium properties deduced from studies of (K^-, K^+) reactions on nuclei in the past [23, 24] or with the aforementioned experimental evidence for possible deeply bound Ξ -hypernuclei [6, 7].

We try to shed some light on this issue in the present work by investigating the properties of the ΞN interaction presented in Ref. [2] in nuclear matter. Specifically, we report results for the single particle (s.p.) potential of the

Ξ hyperon in nuclear matter obtained in a conventional G -matrix calculation based on the standard (gap) choice for the intermediate spectrum. It turns out that the ΞN interaction proposed in Ref. [2], motivated primarily by the intention to show that a BB interaction which fulfills all experimental constraints on $\Lambda\Lambda$ and ΞN scattering can be constructed within chiral EFT, is too repulsive in the medium. However, we will also demonstrate that an updated ΞN interaction can be established that fulfills likewise all experimental constraints on ΞN but yields a moderately attractive Ξ -nuclear potential.

The paper is structured in the following way: In sect. 2 a summary of the employed formalism is provided. We briefly describe the ingredients and the construction of the ΞN interaction within chiral EFT and the equations used for calculating the nuclear matter properties. In sect. 3 we review the results for ΞN scattering of our initial BB interaction [2] and we discuss the properties of an updated version that is proposed in the present study. Subsequently we report results for the pertinent in-medium properties. The paper ends with a brief summary.

2 Formalism

2.1 The YN interaction in chiral EFT

Details of the derivation of the baryon-baryon potentials for the strangeness sector within SU(3) chiral EFT can be found in Refs. [1, 2, 25, 26], see also Ref. [27]. Up to NLO the potentials consist of BB contact terms without derivatives and with two derivatives, together with contributions from one-pseudoscalar-meson exchanges and from (irreducible) two-pseudoscalar-meson exchanges. On the one hand, the contributions from pseudoscalar-meson exchanges (π , η , K) are completely fixed by the assumed SU(3) flavor symmetry. On the other hand, the strength parameters associated with the contact terms, the so-called low-energy constants (LECs), need to be determined in a fit to data. How this is done is described in detail in Ref. [1] for the ΛN and ΣN channels and in Ref. [2] for the BB interaction in the strangeness $S = -2$ sector. In practice, SU(3) flavor symmetry is also used as guideline for the contact terms because this allows one to reduce significantly the number of independent LECs that can contribute. However, it turned out that a consistent description of, for example, NN phase shifts and ΣN scattering data is not possible under the assumption of strict SU(3) symmetry for the contact terms. Because of that, we did not insist on rigorous SU(3) symmetry constraints for the employed LECs, when considering NN and YN or YN and YY [28, 2]. In any case this procedure is fully in line with SU(3) chiral EFT at NLO, because at that order symmetry breaking terms in the leading S -wave contact interactions arise naturally in the perturbative expansion due to meson mass insertions [27].

The chiral BB potential for $S = -2$ up to NLO is described in Ref. [2] and we refer the reader to this paper for details. Here we only want to recall the generic form of the contact interactions because some of the pertinent

LECs will be readjusted in the course of the present study. The contact potentials in the various channels read [1]

$$\begin{aligned} V &= \tilde{C} + C(p^2 + p'^2) \text{ (for } S \text{ waves),} \\ V &= Cpp' \text{ (for } P \text{ waves),} \end{aligned} \quad (1)$$

where p and p' are the center-of-mass (c.m.) momenta in the final and initial state, respectively, and \tilde{C} and C denote the aforementioned LECs that specify the strength of the contact terms. SU(3) symmetry implies that the contact potential in a specific BB channel is given by a particular combination of a basic set of \tilde{C} 's and C 's corresponding to the irreducible SU(3) representations $8 \otimes 8 = 27 \oplus 10^* \oplus 10 \oplus 8_s \oplus 8_a \oplus 1$, relevant for scattering of two octet baryons [29, 30]. The generalized Pauli principle implies that the interaction in partial waves like the 3S_1 , which are symmetric with regard to their spin-space component, is given by linear combinations of LECs corresponding to antisymmetric SU(3) representations (10^* , 10 , 8_a), whereas those with antisymmetric spin-space part (1S_0) receive only contributions from symmetric representations (27 , 8_s , 1). The concrete relations are summarized, e.g., in Table 1 of Ref. [2].

The potentials in the various channels are partial-wave projected [25] and then the reaction amplitudes are obtained from the solution of a coupled-channels Lippmann-Schwinger (LS) equation:

$$\begin{aligned} T_{\nu\nu'}^{\ell'\ell, J}(p'', p'; \sqrt{s}) &= V_{\nu\nu'}^{\ell'\ell, J}(p'', p') \\ &+ \sum_{\ell, \nu} \int_0^\infty \frac{dpp^2}{(2\pi)^3} V_{\nu\nu'}^{\ell''\ell, J}(p'', p) \frac{2\mu_\nu}{k_\nu^2 - p^2 + i\eta} \\ &\times T_{\nu\nu'}^{\ell\ell', J}(p, p'; \sqrt{s}). \end{aligned} \quad (2)$$

The label ν indicates the particle channels and the label ℓ the partial wave. μ_ν is the pertinent reduced mass. The on-shell momentum in the intermediate state, k_ν , is defined by $\sqrt{s} = \sqrt{m_{B_{1,\nu}}^2 + k_\nu^2} + \sqrt{m_{B_{2,\nu}}^2 + k_\nu^2}$. Relativistic kinematics is used for relating the laboratory energy T_{lab} of the hyperons to the c.m. momentum.

In the calculation of phase shifts we solve the LS equation in isospin basis. In this case up to three baryon-baryon channels can couple. For evaluating observables the LS equation is solved in the particle basis, in order to incorporate the correct physical thresholds. Then there are 6 coupled channels for the $\Xi^- p$ system. The potentials in the LS equation are cut off with a regulator function, $f_R(\Lambda) = \exp[-(p^4 + p'^4)/\Lambda^4]$, in order to suppress high-momentum components [31]. Cutoff values in the range $\Lambda = 500 - 650$ MeV are considered, similar to what was used for chiral NN potentials [31]. Following the tradition, we present our results as bands which reflect the variation with the cutoff. These indicate primarily the uncertainty due to the employed regularization scheme. Note that the LECs in the $S = -2$ sector cannot be uniquely determined due to the lack of near-threshold data and, therefore, a genuine uncertainty for the predictions cannot be given at present. This will certainly change in the future, when more data will become available.

2.2 Nuclear matter properties

The nuclear matter properties of the Ξ hyperon are evaluated within the conventional Brueckner theory. We summarize below only the essential elements. A detailed description of the formalism can be found in Refs. [33,32], see also Ref. [34]. We consider the Ξ hyperon with momentum \mathbf{p}_Ξ in nuclear matter at density ρ . In order to determine the in-medium properties of the hyperon we employ the Brueckner reaction-matrix formalism and calculate the ΞN reaction matrix $G_{\Xi N}$, defined by the Bethe-Goldstone equation

$$\langle \Xi N | G(\zeta) | \Xi N \rangle = \langle \Xi N | V | \Xi N \rangle + \sum_{\mathcal{X}} \langle \Xi N | V | \mathcal{X} \rangle \langle \mathcal{X} | \frac{Q}{\zeta - H_0} | \mathcal{X} \rangle \langle \mathcal{X} | G(\zeta) | \Xi N \rangle, \quad (3)$$

with $\mathcal{X} = \Xi N, \Lambda\Lambda, \Lambda\Sigma, \Sigma\Sigma$. Here, Q denotes the Pauli projection operator which excludes intermediate ΞN -states with the nucleon inside the Fermi sea. The starting energy ζ for an initial ΞN -state with momenta \mathbf{p}_Ξ and \mathbf{p}_N is given by

$$\zeta = E_\Xi(p_\Xi) + E_N(p_N), \quad (4)$$

where the single-particle energy $E_\alpha(p_\alpha)$ ($\alpha = \Xi, N$) includes not only the (nonrelativistic) kinetic energy and the baryon mass but in addition the single-particle potential $U_\alpha(p_\alpha, \rho)$:

$$E_\alpha(p_\alpha) = m_\alpha + \frac{\mathbf{p}_\alpha^2}{2m_\alpha} + U_\alpha(p_\alpha, \rho). \quad (5)$$

The conventional 'gap-choice' for the intermediate-state spectrum is adopted. The Ξ single-particle potential $U_\Xi(p_\Xi, \rho)$ is given by the following integral and sum over diagonal ΞN G -matrix elements:

$$U_\Xi(p_\Xi, \rho) = \int_{|\mathbf{p}_N| < k_F} \frac{d^3 p_N}{(2\pi)^3} \text{Tr} \langle \mathbf{p}_\Xi, \mathbf{p}_N | G_{\Xi N}(\zeta) | \mathbf{p}_\Xi, \mathbf{p}_N \rangle, \quad (6)$$

where Tr denotes the trace in spin- and isospin-space. Note that $\rho = 2k_F^3/3\pi^2$ for symmetric nuclear matter considered in the present work, where k_F denotes the Fermi momentum. Eqs. (3) and (6) are solved self-consistently in the standard way, with $U_\Xi(p_\Xi, \rho)$ appearing also in the starting energy ζ . Like in Ref. [35] the nucleon single-particle potential $U_N(p_N, \rho)$ is taken from a calculation of nuclear matter employing a phenomenological NN potential. Specifically, we resort to results for the Argonne v_{18} potential published in Ref. [36]. As pointed out in Ref. [33], calculations of hyperon potentials in nuclear matter using the gap-choice are not too sensitive to the details of $U_N(p_N, \rho)$. Indeed, the difference for $U_\Xi(0, \rho)$ using $U_N(p_N, \rho)$ from Ref. [36] or the parameterization utilized in Ref. [32] amounts to less than 1 MeV at nuclear matter saturation density $\rho = 0.17 \text{ fm}^{-3}$ ($k_F = 1.35 \text{ fm}^{-1}$).

Since at this stage we are only interested in getting a qualitative insight, we refrain from a much more time-consuming calculation necessitated by the so-called 'continuous choice' [37]. A comparison of our leading-order

(LO) results with the ones of Kohno [38] suggests that the continuous choice lowers the Ξ -nuclear potential by roughly 3 MeV at $k_F = 1.35 \text{ fm}^{-1}$. According to Yamamoto et al. [39] the difference (increase in attraction) could be, however, as large as 10 MeV.

3 Results

3.1 ΞN scattering

Our initial study of the baryon-baryon interaction in the strangeness $S = -2$ sector was guided by the aim to meet all the (limited and mostly qualitative) experimental constraints on the $\Lambda\Lambda$ [40,2,41] and ΞN systems [3,5,4]. In practice this meant that we did not take over the employed LECs from our earlier YN study [1] in all cases as it would be compulsory for strict SU(3) symmetry. Rather we exploited the freedom that within SU(3) chiral EFT at NLO symmetry breaking terms in the leading S -wave contact interactions already arise [27]. Specifically, for the 1S_0 partial wave a study of the pp and Σ^+p systems allowed us to quantify the amount of SU(3) symmetry breaking and then infer, in line with SU(3) chiral EFT, the corresponding LEC ($\tilde{C}_{^1S_0}^{27}$) to be used for the $S = -2$ sector [28]. For the LECs in the 3S_1 - 3D_1 partial wave such a procedure was not viable. Therefore, and somewhat arbitrarily the value of $\tilde{C}_{^3S_1}^{8_a}$ was readjusted in the $S = -2$ sector, whereas the other ones ($\tilde{C}_{^3S_1}^{10^*}$ and $\tilde{C}_{^3S_1}^{10}$) were taken over from the YN study [1]. Indeed readjusting that LEC allowed to avoid a near-threshold bound state in the $I = 0$ channel, which arises for the value of $\tilde{C}_{^3S_1}^{8_a}$ fixed in the fit to YN data and which is the main reason why the Ξ^-p cross section based on the LECs from our YN study exceeds the upper limits set by experiments [4] dramatically, see the extensive discussion in Ref. [2].

As we will show below, the ΞN interaction fixed in that way leads to unrealistic in-medium properties. Specifically, the s.p. potential for the Ξ turns out to be much too repulsive. Therefore, in the present paper we seek for an alternative solution, where now we allow variations of the LECs $\tilde{C}_{^3S_1}^{10^*}$ and $\tilde{C}_{^3S_1}^{10}$ too. Our aim is to explore the possibility to establish a ΞN interaction that still meets all the experimental constraints for $\Lambda\Lambda$ and ΞN scattering, but at the same time implies an attractive Ξ s.p. potential. Thereby, the interaction in the 1S_0 partial wave is taken over from our previous work [2]. After all, our predictions for $\Lambda\Lambda$ and $\Xi N \rightarrow \Lambda\Lambda$ are well in line with experiments and, moreover, they are supported by the latest (though still preliminary) results from lattice QCD simulations [18]. The latter is also the case for the ΞN 3S_1 - 3D_1 interaction in the isospin $I = 0$ channel so that we simply take over the values for $\tilde{C}_{^3S_1}^{8_a}$ fixed in Ref. [2].

Results for those ΞN channels where data are available are presented in Fig. 1. Here the hatched bands are the NLO results from Ref. [2] and the black/red bands those of the new alternative solution. For illustration we include also predictions obtained at leading order (LO) [26], cf. the light (green) bands. As already said above, the results

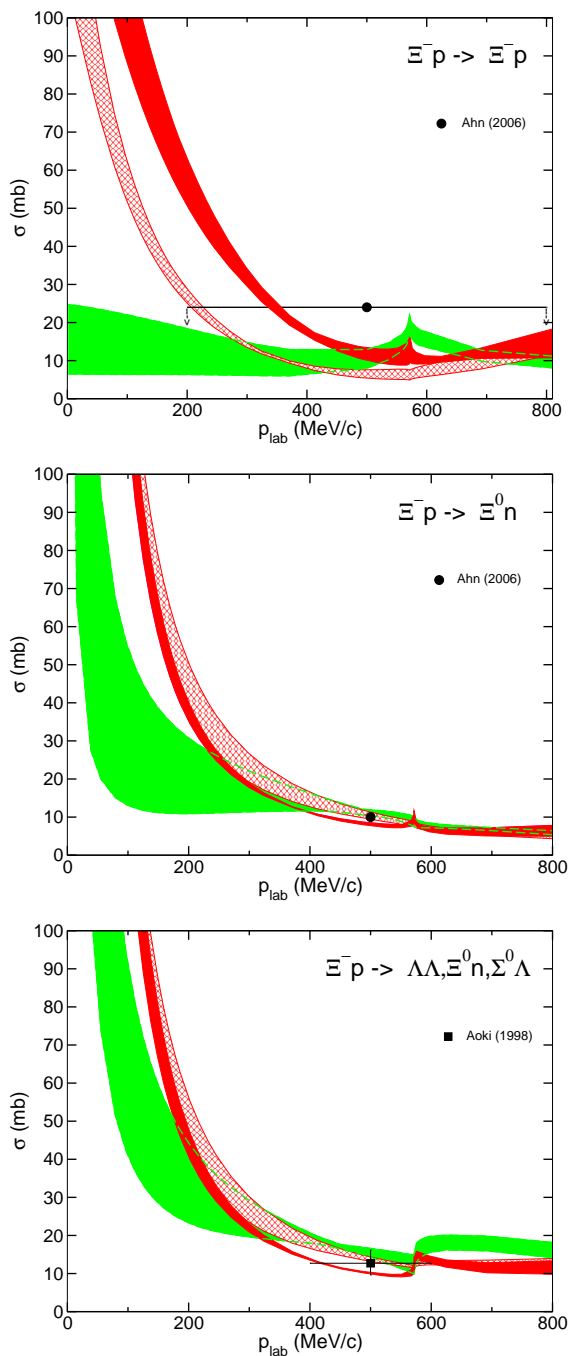


Fig. 1. $\Xi^- p$ induced cross sections. The black/red bands represent results at NLO, based on the new fit with readjusted LECs $\tilde{C}_{3S_1}^{10^*}$ and $\tilde{C}_{3S_1}^{10}$, see text. The hatched bands are results for the NLO interaction from Ref. [2] while the grey/green bands are those from a LO calculation [26]. Experiments are from Ahn et al. [4] and Aoki et al. [5].

for the $\Lambda\Lambda \rightarrow \Lambda\Lambda$ and $\Xi^- p \rightarrow \Lambda\Lambda$ cross sections remain unchanged and, therefore, are not reproduced here.

As visible in Fig. 1, the main difference between the ΞN interaction from Ref. [2] and the new fit is that in the former the $\Xi^- p$ elastic cross section remains strictly below the upper bound while now the limit provided by the experiment is fulfilled only in average over the given mo-

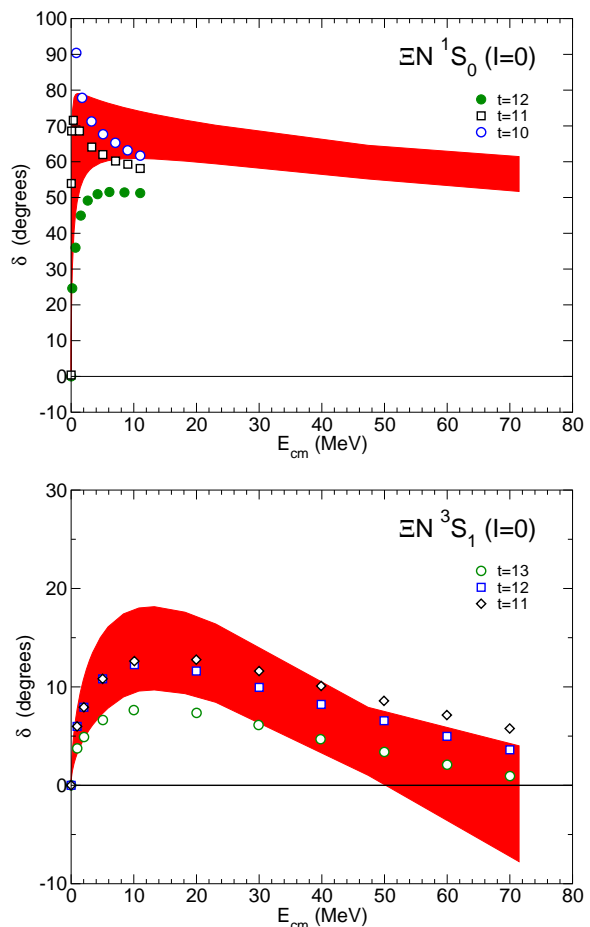


Fig. 2. ΞN isospin $I = 0$ phase shifts from Ref. [2]. The symbols indicate preliminary results from lattice QCD calculations by the HAL QCD collaboration for different sink-source time-separations t [18].

mentum range of $200 < p_{\text{lab}} < 800$ MeV/c. Both scenarios are, of course, consistent with the empirical findings [4]. The phase shifts in the ΞN S -waves are summarized in Figs. 2 and 3. For completeness we show here all S -waves though the alternative solution concerns only the 3S_1 - 3D_1 partial wave with $I = 1$. One can see that now the interaction in the latter partial wave is moderately attractive while it was basically repulsive in our previous work [2]. Interestingly, this attraction leads to a much more pronounced cusp effect at the opening of the $\Lambda\Sigma$ channel, comparable to what happens in the ΛN case at the opening of the ΣN channel [1,42].

Table 1 provides a summary of the pertinent S -wave effective range parameters. Besides the ones of our chiral EFT interactions we included values for two phenomenological potential models from the literature, whose G -matrix results will serve us as benchmark in the discussion of in-medium properties below. The models in question are the Nijmegen ESC08c meson-exchange potential [22] and the quark-model potential fss2 [43]. Note that the large and positive value of a_{3S_1} for $I = 1$ in case of the Nijmegen ESC08c potential indicates the presence of a bound state

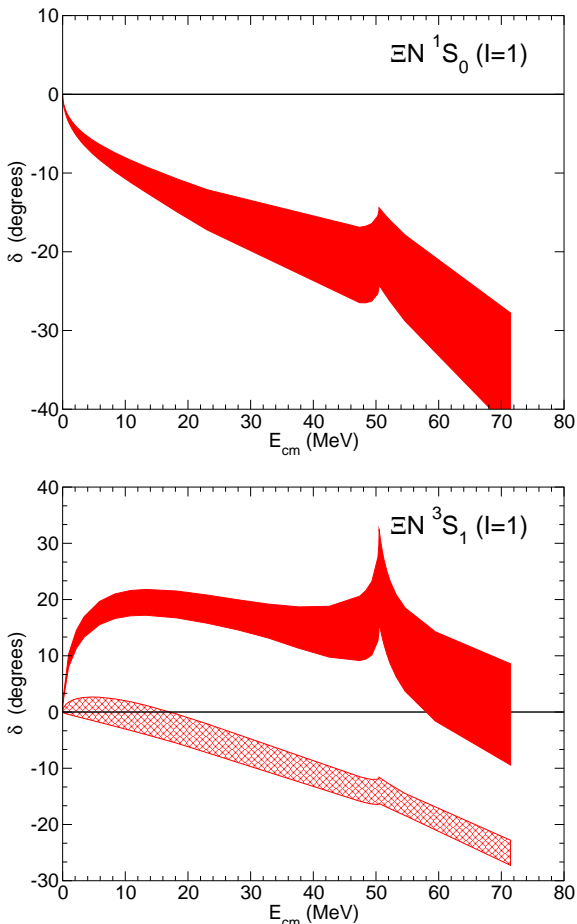


Fig. 3. ΞN isospin $I = 1$ phase shifts. The hatched band are the 3S_1 phase shifts for the interaction presented in Ref. [2]. The full band represents the one for the updated ΞN interaction considered in the present work.

in this partial waves. A more comprehensive overview of ΞN effective range parameters predicted over the years can be found in Ref. [40].

As already mentioned, recently lattice QCD results close to the physical point ($M_\pi = 146$ MeV) have become available for the $S = -2$ sector from the HAL QCD Collaboration [18,19]. The reported phase shifts for the ΞN 1S_0 and 3S_1 partial waves with isospin $I = 0$ are very similar to the ones predicted by our EFT interaction earlier [2]. This can be seen in Fig. 2, where the phases from the lattice are included for illustration. We want to emphasize, however, that the HAL QCD results are still preliminary. Also, we show here only the central values for different sink-source time-separations t [44]. For the pertinent statistical errors see Ref. [18]. In any case, one interesting aspect is that the present lattice results support the possible existence of a virtual state in the $I = 0$ 1S_0 partial wave very close to the ΞN threshold, predicted in [2], which can be considered as a remnant of the H -dibaryon [45,46]. It is reflected in large values of the corresponding ΞN phase shifts, see upper panel of Fig. 2, and large negative values of the scattering length, cf. Table 1. It is also

worthwhile mentioning that the HAL QCD lattice simulations suggest values around -0.65 fm for $a_{3S_1}^{I=0}$ [18], which is well within the range predicted by our NLO potential [2].

3.2 Ξ in nuclear matter

The properties of our ΞN interaction in nuclear matter are documented in Table 3 and Fig. 4. The table summarizes the results for the Ξ potential depth, $U_\Xi(p_\Xi = 0)$, evaluated at the saturation point of nuclear matter, i.e. for $k_F = 1.35$ fm $^{-1}$, for the NLO interaction of Ref. [2] and the updated interaction considered in the present study. For completeness we include also an exemplary result for our LO potential [26]. In addition, results for two potentials from the literature are listed, namely for the Nijmegen ESC08c potential [22] and the quark-model based potential fss2 [43].

There are indications for a moderately attractive in-medium ΞN interaction, as already pointed out in the Introduction. In particular, a strength of $U_\Xi \approx -14$ MeV for the Ξ -nucleus potential is considered as the benchmark now [47]. This value was deduced from the initial analysis of the BNL-E885 measurement of the spectrum of the (K^-, K^+) reaction on a ${}^{12}\text{C}$ target based on a Woods-Saxon potential [23]. Since we calculate the Ξ -nuclear potential in infinite nuclear matter we should, however, not really compare our result directly with that figure. At least this is suggested by investigations in the literature where G -matrix calculations similar to ours were presented and where, in addition, analyses of finite Ξ systems were performed utilizing Ξ -nucleus potentials derived from those G -matrices. For instance, in studies based on the Nijmegen ESC08 potentials [22,13] predictions for Ξ -hypernuclei were reported which are apparently consistent with the indications of the BNL experiment [23] and with the Kiso event [6]. However, if we take exemplary the ESC08c model, the corresponding potential in nuclear matter, evaluated at saturation density, amounts to -7 MeV only [22]. In the analysis by Kohno and Hashimoto [48] (see also Ref. [49]) that is partly based on the quark-model potential fss2 [43] the authors came likewise to the conclusion that the BNL data do not necessarily imply an attractive Ξ -nucleus potential in the order of 14 MeV. Indeed, in this work it is concluded that an almost zero potential is preferable.

Table 3 reveals what has been already anticipated in subsect. 3.1: The original NLO interaction [2] with LECs fixed solely with the aim to meet the available experimental constraints on $\Xi^- p$ scattering leads to unrealistic strongly repulsive predictions for the Ξ s.p. potential. However, the updated NLO interaction presented here makes clear that it is possible to maintain agreement with those constraints and, at the same time, achieve a moderately attractive Ξ -nuclear interaction. Evidently, the values we obtain for $U_\Xi(0)$ are smaller than the commonly cited benchmark based on the original fit to the BNL data [23]. Yet, they are comparable to the results for the ΞN

Table 1. ΞN scattering lengths and effective ranges (in fm) for the NLO potential for cutoffs $\Lambda = 500 - 650$ MeV. Results for the interaction considered in Ref. [2] are shown in brackets when different. Values for the Nijmegen ESC08c potential [22] and from the quark-model potential fss2 [43] are included too.

	1S_0			3S_1			
	$I = 0$	$I = 1$		$I = 0$		$I = 1$	
potential	a	a	r	a	r	a	r
NLO (500)	$-7.71 - i 2.03$	0.37	-4.80	-0.33	-6.86	-1.17	3.44
						(-0.20	35.6)
NLO (550)	$-7.24 - i 20.79$	0.39	-4.95	-0.39	-1.77	-1.15	3.80
						(-0.04	575)
NLO (600)	$-10.89 - i 14.91$	0.34	-7.20	-0.62	1.00	-1.13	3.95
						(0.02	1797)
NLO (650)	$-8.14 - i 2.43$	0.31	-9.16	-0.85	1.42	-0.90	4.27
						(0.04	450)
ESC08c		0.58	-2.52	-5.36	1.43	4.91	0.53
fss2				0.32	-8.93	-0.21	26.2

Table 2. New values of the LECs in the 3S_1 partial wave for the considered cutoffs Λ , in the notation of Ref. [2]. In addition $C_{^3P_0}^{8s} = -0.5$ and $C_{^3P_2}^{8s} = -0.15$ are used in the alternative NLO fit. The values for \tilde{C} are in 10^4 GeV^{-2} , those for the C 's in 10^4 GeV^{-4} .

Λ [MeV]	500	550	600	650
$\tilde{C}_{^3S_1}^{10*}$	0.541	1.49	1.64	2.40
$\tilde{C}_{^3S_1}^{10}$	0.011	0.05	0.62	1.20

potentials ESC08c and fss2, for which likewise consistency with those BNL data is claimed.

As mentioned, for simplicity reasons we have performed the G -matrix calculation with the gap choice. However, we expect additional attraction in the order of 3 MeV or more for the continuous choice, cf. the comments in subsect. 2.2, which means that our results for $U_{\Xi}(0)$ are indeed very similar to those of the ESC08c potential. Nonetheless it is important to note that, contrary to that model, our EFT interaction meets all the available empirical constraints on the $\Lambda\Lambda$ and ΞN interactions, see subsect. 3.1 and Ref. [2]. Specifically, it does not lead to a near-threshold bound state in the 3S_1 - 3D_1 partial wave of the ΞN $I = 1$ channel. The existence of such a state is practically excluded by the mentioned experimental constraints [2], and it is also not supported by the latest lattice QCD simulations close to the physical point [20].

It should not be concealed that a considerable uncertainty in the predictions for the Ξ s.p. potential comes from the contributions of the P -waves. Since there is very little information on angular-dependent observables for ΛN and ΣN and none for ΞN , the pertinent LECs cannot

be directly adjusted to data. Their values have been fixed in our works [1,2] essentially by requiring that the contributions of the P -waves to the Λp and ΞN cross sections

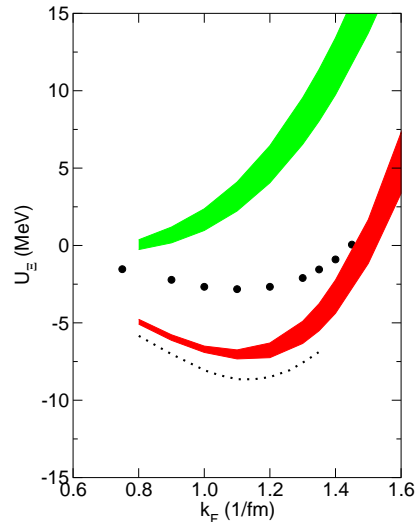


Fig. 4. The Ξ s.p. potential $U_{\Xi}(p_{\Xi} = 0)$ as a function of the Fermi momentum k_F . The black/red band shows the chiral EFT results to NLO for variations of the cutoff in the range $\Lambda = 500, \dots, 650$ MeV. The outcome at LO is indicated by the grey/green band. The dotted line is the result for the Nijmegen potential ESC08c [22], the circles those for the quark-model potential fss2 [43], taken from Ref. [38].

Table 3. Results for Ξ in nuclear matter. Partial wave contributions to $U_{\Xi}(p_{\Xi} = 0)$ (in MeV) at the Fermi momentum $k_F = 1.35 \text{ fm}^{-1}$, for the LO [26] and NLO interactions for various cutoffs. NLO* indicates the NLO interaction from Ref. [2]. Results for the Nijmegen ESC08c potential are taken from Ref. [22], those for the quark-model potential fss2 from Ref. [48].

potential	I	1S_0	3S_1	3P_0	1P_1	3P_1	3P_2	S -waves	total
NLO (500)	0	-2.6	-3.3	-0.7	-0.9	1.7	-0.6		
	1	12.7	-11.8	1.4	1.5	-0.3	-2.5	-5.0	-5.5
NLO (550)	0	-2.9	-3.1	-0.7	-0.9	1.7	-0.6		
	1	12.4	-9.5	1.3	1.4	-0.4	-2.5	-3.1	-3.8
NLO (600)	0	-2.9	-3.8	-0.8	-0.9	1.7	-0.6		
	1	10.4	-7.0	1.3	1.4	-0.5	-2.6	-3.3	-4.3
NLO (650)	0	-2.7	-4.8	-0.8	-1.0	1.6	-0.6		
	1	9.1	-4.1	1.2	1.3	-0.6	-2.7	-2.5	-4.1
NLO*(500)	0	-3.1	-3.3	-0.5	-0.9	1.7	0.1		
	1	11.4	9.1	3.1	1.5	-0.4	4.4	14.1	23.1
NLO*(550)	0	-3.6	-3.2	-0.5	-0.9	1.7	0.1		
	1	10.9	16.0	2.7	1.4	-0.4	3.8	20.1	27.7
NLO*(600)	0	-3.5	-4.1	-0.6	-1.0	1.7	0.0		
	1	9.0	18.0	2.4	1.4	-0.5	3.2	19.4	26.0
NLO*(650)	0	-3.2	-5.2	-0.6	-1.0	1.6	-0.1		
	1	8.0	17.2	2.2	1.3	-0.7	2.8	17.0	22.4
LO (600)	0	-1.2	-4.9	-1.1	-0.5	1.7	-0.3		
	1	6.8	9.8	1.1	0.9	-3.1	0.2	10.5	9.3
ESC08c	0	1.4	-8.0	1.8	-0.3	1.4	-2.1		
	1	10.7	-11.1	0.7	1.1	-2.6	-0.0	-7.0	-7.0
fss2									-1.5

remain small with increasing energy, to be in line with the experiment. Of course, this prescription does not fix the sign, i.e. does not allow to determine whether the interactions in question are repulsive or attractive. We see from the results for U_{Ξ} in Table 3 that in case of the original NLO interaction about 25 % of the repulsion is generated by the P -waves. On the other hand, in case of the LO(600) interaction and the Nijmegen ESC08c potential the P -wave contributions cancel more or less and the total result is practically given by that of the S -waves alone. In other versions of the Nijmegen potential [39] and also in other ΞN potentials [50] the P -waves provide even additional attraction in the order of 5 MeV. Because of that in the updated NLO interaction we have tried to achieve a balance between the P -wave contributions by readjusting some of the pertinent LECs, see Table 2 for details. In addition the sum of the S -wave contributions is listed separately in the table. Those are the ones which are primarily constrained by the available empirical information on the ΞN interaction.

Predictions for the density dependence of the Ξ s.p. potential are presented in Fig. 4 where $U_{\Xi}(0)$ is shown as a function of k_F for the updated NLO potential. Results for the LO interaction are shown too and, for the ease of comparison, those for the ESC08c and fss2 potentials. Interestingly, the updated NLO interaction and the ESC08c potential exhibit a very similar density dependence. In particular, there is a trend towards repulsion with increasing density – and in case of the NLO interaction the change of sign of U_{Ξ} occurs already at rather moderate nuclear matter density. Accordingly, one expects that the onset density for the appearance of the Ξ hyperons in neutron stars should be fairly high for such interactions [13], and, in turn, there should be a rather small effect on the equation-of-state [9,10]

4 Summary

We have investigated the in-medium properties of baryon-baryon potentials for the strangeness $S = -2$ sector, derived within chiral effective field theory up to next-to-

leading order and constrained by available experimental information on the $\Lambda\Lambda$ and ΞN systems. In particular, we have evaluated the single-particle potential for the Ξ hyperon in nuclear matter in a conventional G -matrix calculation.

We could show that a ΞN interaction can be constructed which is in line with empirical constraints on the $\Lambda\Lambda$ S -wave scattering length and with published values and upper bounds for Ξ^-p elastic and inelastic cross sections and which, at the same time, yields a moderately attractive Ξ -nuclear interaction as suggested by recent experimental evidence for the existence of Ξ -hypernuclei [6, 8]. The values obtained for the Ξ single-particle potential $U_{\Xi}(0)$ in nuclear matter are with -3 to -5 MeV somewhat smaller than the commonly cited potential depth of -14 MeV. However, they are in line with results from comparable G -matrix calculations based on phenomenological ΞN potentials, where in applications to finite Ξ systems consistency with data such as the spectrum in the $^{12}\text{C}(K^-, K^+)X$ reaction [23] has been claimed [48, 22]. It is also found that the original ΞN interaction published in Ref. [2], which was primarily meant to demonstrate that a baryon-baryon interaction fulfilling all experimental constraints on $\Lambda\Lambda$ and ΞN scattering can be established, is too repulsive in the medium.

Of course, one has to acknowledge that the nuclear matter calculations we performed can provide only a first insight into the properties of the ΞN interaction in the medium. A more stringent test of those properties could be achieved by deducing effective interactions (from the G -matrix in nuclear matter) and applying them in calculations of finite hypernuclei. Such a much more challenging investigation is postponed to the future.

Finally, we want to emphasize that also for the updated NLO ΞN interaction introduced in the present paper no elaborate fine-tuning of the low-energy constants associated with the contact terms has been attempted. For that one has to wait for further and more quantitative constraints from experiments involving the Ξ hyperon and/or possibly employ [51] predictions from lattice QCD simulations [20] once final and confirmed results become available. Further experimental information could come from future experiments involving the Ξ hyperon at J-PARC [52] or FAIR [53], but also from the study of pertinent correlations in heavy ion collisions or in high-energetic pp scattering [15].

Acknowledgments

This work is supported in part by the DFG and the NSFC through funds provided to the Sino-German CRC 110 ‘‘Symmetries and the Emergence of Structure in QCD’’ (DFG grant. no. TRR 110) and the VolkswagenStiftung (grant no. 93562). The work of UGM was supported in part by The Chinese Academy of Sciences (CAS) President’s International Fellowship Initiative (PIFI) (grant no. 2018DM0034).

References

1. J. Haidenbauer, S. Petschauer, N. Kaiser, U.-G. Meißner, A. Nogga and W. Weise, Nucl. Phys. A **915**, 24 (2013).
2. J. Haidenbauer, U.-G. Meißner and S. Petschauer, Nucl. Phys. A **954**, 273 (2016).
3. J. K. Ahn *et al.* [E224 Collaboration], Nucl. Phys. A **625**, 231 (1997).
4. J. K. Ahn *et al.*, Phys. Lett. B **633** (2006) 214.
5. S. Aoki *et al.*, Nucl. Phys. A **644**, 365 (1998).
6. K. Nakazawa *et al.*, PTEP **2015**, 033D02 (2015).
7. T. Nagae *et al.*, PoS INPC **2016**, 038 (2017).
8. T. Nagae, *The 13th International Conference on Hypernuclear and Strange Particle Physics, June 24-29, 2018, Portsmouth, USA*, https://www.jlab.org/conferences/hyp2018/talks/wed/am/04_nagae.pdf
9. S. Weissenborn, D. Chatterjee, and J. Schaffner-Bielich, Nucl. Phys. A **881** (2012) 62.
10. S. Weissenborn, D. Chatterjee, and J. Schaffner-Bielich, Phys. Rev. C **85** (2012) 065802.
11. T. Katayama and K. Saito, Phys. Lett. B **747**, 43 (2015)
12. D. Chatterjee and I. Vidaña, Eur. Phys. J. A **52**, 29 (2016)
13. Y. Yamamoto, T. Furumoto, N. Yasutake and T. A. Rijken, Eur. Phys. J. A **52**, 19 (2016).
14. L. Tolos, M. Centelles and A. Ramos, Astrophys. J. **834**, 3 (2017).
15. L. Fabbietti, *The 13th International Conference on Hypernuclear and Strange Particle Physics, Portsmouth, USA, June 2018*, <https://www.jlab.org/conferences/hyp2018/program.html>
16. T. Hatsuda, K. Morita, A. Ohnishi and K. Sasaki, Nucl. Phys. A **967**, 856 (2017).
17. J. Haidenbauer, arXiv:1808.05049 [hep-ph].
18. K. Sasaki, presentation at the 35th International Symposium on Lattice Field Theory, Lattice2017, 18-24 June 2017, Granada, Spain, <https://makondo.ugr.es/event/0/session/94/contribution/72/material/slides/1.pdf>
19. K. Sasaki *et al.* [HAL QCD Collaboration], EPJ Web Conf. **175**, 05010 (2018).
20. T. Inoue, arXiv:1809.08932.
21. T. A. Rijken, M.M. Nagels, Y. Yamamoto, Prog. Theor. Phys. Suppl. **185**, 14 (2010).
22. M. M. Nagels, T. A. Rijken and Y. Yamamoto, arXiv:1504.02634 [nucl-th].
23. P. Khaustov *et al.* [AGS E885 Collaboration], Phys. Rev. C **61**, 054603 (2000).
24. T. Fukuda *et al.* [E224 Collaboration], Phys. Rev. C **58**, 1306 (1998).
25. H. Polinder, J. Haidenbauer, U.-G. Meißner, Nucl. Phys. A **779**, 244 (2006).
26. H. Polinder, J. Haidenbauer, U.-G. Meißner, Phys. Lett. B **653**, 29 (2007).
27. S. Petschauer and N. Kaiser, Nucl. Phys. A **916**, 1 (2013).
28. J. Haidenbauer, U.-G. Meißner and S. Petschauer, Eur. Phys. J. A **51**, 17 (2015).
29. J. J. de Swart, Rev. Mod. Phys. **35**, 916 (1963).
30. C. B. Dover and H. Feshbach, Annals Phys. **198**, 321 (1990).
31. E. Epelbaum, W. Glöckle, U.-G. Meißner, Nucl. Phys. A **747**, 362 (2005).

32. J. Haidenbauer, U.-G. Meißner, Nucl. Phys. A **936**, 29 (2015).
33. A. Reuber, K. Holinde, J. Speth, Nucl. Phys. A **570**, 543 (1994).
34. I. Vidaña, A. Polls, A. Ramos, M. Hjorth-Jensen and V. G. J. Stoks, Phys. Rev. C **61** (2000) 025802.
35. J. Haidenbauer, U.-G. Meißner, N. Kaiser and W. Weise, Eur. Phys. J. A **53**, 121 (2017).
36. F. Isaule, H. F. Arellano and A. Rios, Phys. Rev. C **94**, 034004 (2016).
37. S. Petschauer, J. Haidenbauer, N. Kaiser, U.-G. Meißner, W. Weise, Eur. Phys. J. A **52**, 15 (2016).
38. M. Kohno, Phys. Rev. C **81**, 014603 (2010).
39. Y. Yamamoto, T. Motoba and T. A. Rijken, Prog. Theor. Phys. Suppl. **185**, 72 (2010).
40. A. M. Gasparyan, J. Haidenbauer and C. Hanhart, Phys. Rev. C **85**, 015204 (2012).
41. A. Ohnishi, K. Morita, K. Miyahara and T. Hyodo, Nucl. Phys. A **954**, 294 (2016).
42. H. Machner et al., Nucl. Phys. A **901**, 65 (2013).
43. Y. Fujiwara, Y. Suzuki, C. Nakamoto, Prog. Part. Nucl. Phys. **58**, 439 (2007).
44. N. Ishii *et al.* [HAL QCD Collaboration], Phys. Lett. B **712**, 437 (2012).
45. J. Haidenbauer and U.-G. Meißner, Phys. Lett. B **706**, 100 (2011).
46. J. Haidenbauer and U.-G. Meißner, Nucl. Phys. A **881**, 44 (2012).
47. A. Gal, E. V. Hungerford and D. J. Millener, Rev. Mod. Phys. **88**, 035004 (2016).
48. M. Kohno and S. Hashimoto, Prog. Theor. Phys. **123**, 157 (2010).
49. M. Kohno and Y. Fujiwara, Phys. Rev. C **79**, 054318 (2009).
50. M. Yamaguchi, K. Tominaga, T. Ueda and Y. Yamamoto, Prog. Theor. Phys. **105**, 627 (2001).
51. K.-W. Li, T. Hyodo and L.-S. Geng, arXiv:1809.03199 [nucl-th].
52. T. Nagae et al., http://j-parc.jp/researcher/Hadron/en/pac_1801/pdf/P70_2018-10.pdf
53. A. Sanchez Lorente [PANDA Collaboration], Hyperfine Interact. **229**, 45 (2014).